iScience

CellPress
OPEN ACCESS

Article

BCG Vaccinations Upregulate Myc, a Central Switch for Improved Glucose Metabolism in Diabetes

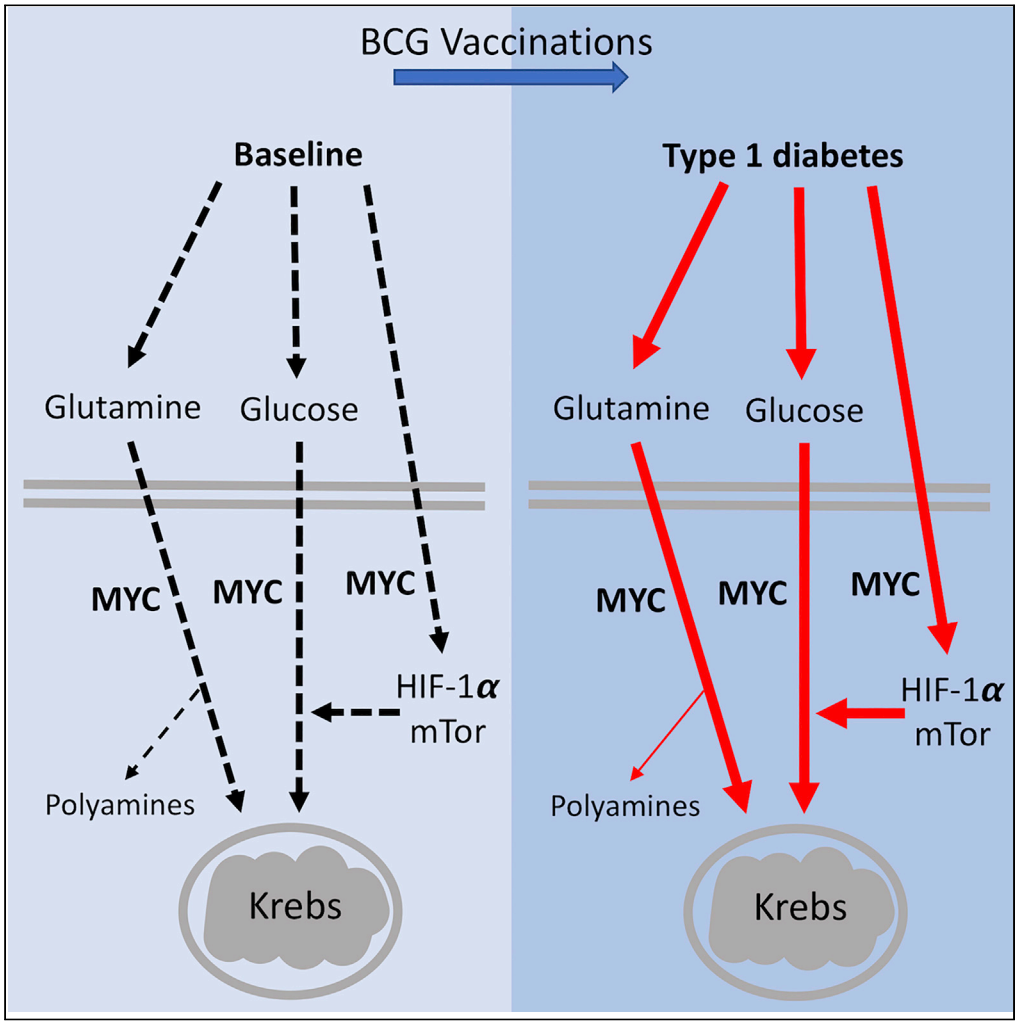

Willem M. Kühtreiber, Hiroyuki Takahashi, Ryan C. Keefe, ..., Sarah M. Sinton, Jessica C. Graham, Denise L. Faustman

faustman@helix.mgh.harvard.edu

HIGHLIGHTS

T1D has insufficient aerobic glycolysis; this causes insufficient sugar utilization

BCG vaccine lowers blood sugar levels in T1D by augmenting aerobic glycolysis

BCG-induced shift to aerobic glycolysis is associated with Myc activation

Host-microbe BCG interactions through Myc activate sugar-regulating genes in T1D

Kühtreiber et al., iScience *23*, 101085
May 22, 2020
https://doi.org/10.1016/j.isci.2020.101085

iScience

CellPress
OPEN ACCESS

Article

BCG Vaccinations Upregulate Myc, a Central Switch for Improved Glucose Metabolism in Diabetes

Willem M. Kühtreiber,[1] Hiroyuki Takahashi,[1] Ryan C. Keefe,[1] Yaerin Song,[1] Lisa Tran,[1] Trevor G. Luck,[1] Gabriella Shpilsky,[1] Louisa Moore,[1] Sarah M. Sinton,[1] Jessica C. Graham,[1] and Denise L. Faustman[1,2,*]

SUMMARY

Myc has emerged as a pivotal transcription factor for four metabolic pathways: aerobic glycolysis, glutaminolysis, polyamine synthesis, and HIF-1α/mTOR. Each of these pathways accelerates the utilization of sugar. The BCG vaccine, a derivative of *Mycobacteria-bovis*, has been shown to trigger a long-term correction of blood sugar levels to near normal in type 1 diabetics (T1D). Here we reveal the underlying mechanisms behind this beneficial microbe-host interaction. We show that baseline glucose transport is deficient in T1D monocytes but is improved by BCG *in vitro* and *in vivo*. We then show, using RNAseq in monocytes and CD4 T cells, that BCG treatment over 56 weeks in humans is associated with upregulation of Myc and activation of nearly two dozen Myc-target genes underlying the four metabolic pathways. This is the first documentation of BCG induction of Myc and its association with systemic blood sugar control in a chronic disease like diabetes.

INTRODUCTION

Several metabolic pathways are central to aerobic glycolysis, the process of accelerated utilization of extracellular glucose instead of the less glucose-dependent process of oxidative phosphorylation (OXPHOS) and the Krebs cycle. Myc, also known as c-Myc, is a family of regulator genes that code for transcription factors that play a major intracellular role in glucose homeostasis (Lewis et al., 1997). Myc's pivotal role in the control of sugar metabolism first emerged as central target genes were identified in sugar transport and glycolysis, such as involvement of lactate dehydrogenase (LDH) (Ramanathan et al., 2005; Shim et al., 1997). Myc-regulated glycolysis utilizes lactate dehydrogenase A (LDHA), which converts pyruvate to lactate as part of the glycolytic pathway. This research evolved into the subsequent identification of 20 putative Myc target genes in the glycolysis pathway (Dang et al., 2009). Myc upregulates glucose transporter GLUT1, hexokinase 2 (HK2), phosphofructokinase (PFKM), and enolase 1 (ENO1) (Osthus et al., 2000). Through upregulation of these genes, Myc was effectively contributing heavily to the entire direct multistep process of aerobic glycolysis, a high cellular glucose utilization state. It is now appreciated that Myc is so central to aerobic glycolysis that nearly all genes encoding glycolytic enzymes are direct Myc targets and are under Myc control (Dang et al., 2006; Guo et al., 2000; Kim and Dang, 2006).

The metabolic pathways under Myc control include glycolysis, glutaminolysis, and polyamine synthesis (Le et al., 2012). Ornithine decarboxylase, which promotes polyamine synthesis, is a Myc trigger (Nilsson et al., 2005). Glutamine metabolism is a complementary pathway to glycolysis and coordinates increased amino acids, lipids, and nucleotide biosynthesis while also providing energy to support these processes. Myc regulates glutaminolysis for cell metabolism at multiple levels of sequential gene induction. It is important to note that Myc regulates both glycolysis and glutaminolysis. Polyamine synthesis is also under Myc control.

It has recently become appreciated that host-microbe interactions result in dramatic changes in cellular metabolism often toward accelerated aerobic glycolysis. Some microorganisms utilize host toll-like receptor 4 (TLR4) or lipopolysaccharide (LPS) external stimuli to alter target cell metabolism toward glycolysis with or without suppression of OXPHOS (Palsson-McDermott et al., 2015; Rodríguez-Prados et al., 2010; Ruiz-García et al., 2011; Tan et al., 2015). Other microorganisms appear to drive whole organisms to both accelerated glycolysis and OXPHOS in human monocytes through TLR2 receptors, such as through

[1]Immunobiology Laboratories, Harvard Medical School & Massachusetts General Hospital, Building 149, 13th Street, Rm 3602, Boston, MA 02116, USA

[2]Lead Contact

*Correspondence: faustman@helix.mgh.harvard.edu

https://doi.org/10.1016/j.isci.2020.101085

P3C cell wall component exposures (Lachmandas et al., 2016). And, lastly, β-glucan, a fungal derivative, uses the Dectin-1 receptor for host-induced glycolysis, increasing both glutamine and cholesterol synthesis. In general, many microorganisms or their cell wall components can promote a shift in host metabolism to reliance on glucose as an energy source, a switch to aerobic glycolysis. As more data have accumulated it has become apparent that not all microorganisms stimulate this switch to aerobic glycolysis through the same host intracellular pathways (Everts et al., 2014; Kelly and O'Neill, 2015; Krawczyk et al., 2010; Rodríguez-Prados et al., 2010; Stienstra et al., 2017). It is important in the case of type 1 diabetes (T1D), where improved sugar utilization is desired to understand the monocyte and T cell pathways that might be augmented by beneficial reintroduction of microbes such as by vaccination with bacillus calmette guerin (BCG).

The introduction of BCG, a >100-year-old vaccine and a derivative of *Mycobacterium bovis*, given in two doses to T1D adults resulted in the recovery of tight and long-lasting blood sugar control during an 8-year long human study (Kühtreiber et al., 2018). The mechanism underlying this benefit was not only by increase in more beneficial immune cells such as suppressive regulatory T cells (Tregs) through changes in BCG-controlled methylation patterns but also by a systemic restoration of proper glucose metabolism through aerobic glycolysis (Kühtreiber et al., 2018). These findings were based on a double-blind randomized controlled clinical trial using two repeat BCG vaccines and tracking of patients for several years before long-lasting changes in metabolism were sufficient to control blood sugars (Faustman et al., 2012). BCG was found to shift cellular metabolism to optimize sugar energy sources, to use the pentose phosphate shunt, and to turn off OXPHOS (Kühtreiber et al., 2018). In tuberculosis, the pathologic version of the BCG vaccine, these effects were observed in the lung tuberculosis granuloma in a murine model (Shi et al., 2015). With repeat BCG vaccinations via intradermal injection in humans a systemic shift occurs; this shift can be monitored by sampling lymphocytes obtained from the peripheral blood for direct sugar uptake rates. Global data suggest that many microorganisms that infect humans optimize energy metabolism by shifting the host to sugar metabolism from low sugar utilization energy states such as OXPHOS to high glucose utilization states. High sugar utilization states appear to contribute to a meaningful contribution to glucose homeostasis.

Why do TID patients have underlying defects in glucose transport? They may be due to insufficient host-microbe interactions, a concept supported by the hygiene hypothesis (Kühtreiber and Faustman, 2019). The hygiene hypothesis asserts that all forms of autoimmunity and allergies are more prevalent in cultures and societies with minimal bacterial interactions due to cleanliness, lack of well water as a source of mycobacteria, and movement from an agrarian culture to a "clean" suburban location (Bach, 2002; Strachan, 1989). Indeed it has been noted that high tuberculosis mycobacteria burden in populations protects against T1D and other autoimmune diseases (Airaghi and Tedeschi, 2006; Andersen et al., 1981). Also dramatic shifts in autoimmune disease incidence can occur with changes in the environmental microbe exposure, as evidenced by a 6-fold gradient in T1D burden between eastern Finland and nearby Russia from recently separated populations (Kondrashova et al., 2005).

Recent *in vitro* data have begun to show how microorganisms reset host metabolism. This reset can occur at the gene level through epigenetic imprinting, at the mRNA level, and ultimately by monitoring gradual alteration of metabolites in the serum. Terms such as "trained immunity" and "old friends" apply to epigenetic host-microbe changes that benefit both host and microbe (Bloomfield et al., 2016; Netea et al., 2016). Ultimately the major cellular readout for confirmed physiological relevance is increased glucose uptake by T cells or monocytes regardless of the gene, mRNA, phosphorylation, or protein modifications conferred by the beneficial re-introduction of these ancient organisms that co-evolved with humans until recently (Brites and Gagneux, 2015; Kodaman et al., 2014). It should be noted that BCG effects, as observed in these reported results, are not confined to only innate cells such as monocytes but also extend to T cells as part of the adaptive immune response as well, thus broading the impact of BCG to both limbs of the immune system.

Here we present a basic science study of diabetic humans receiving repeat BCG vaccines. We explore the role of Myc control of glycolysis, glutaminolysis, polyamine synthesis, and the hypoxia-inducible factor (HIF)-1α/mTOR pathway. Human subjects are monitored *in vivo* and *in vitro* at serial time points spanning at least one year during receipt of three BCG vaccinations. This study represents one step closer to understanding beneficial host-microbe interactions that involve metabolic corrections affecting sugar utilization.

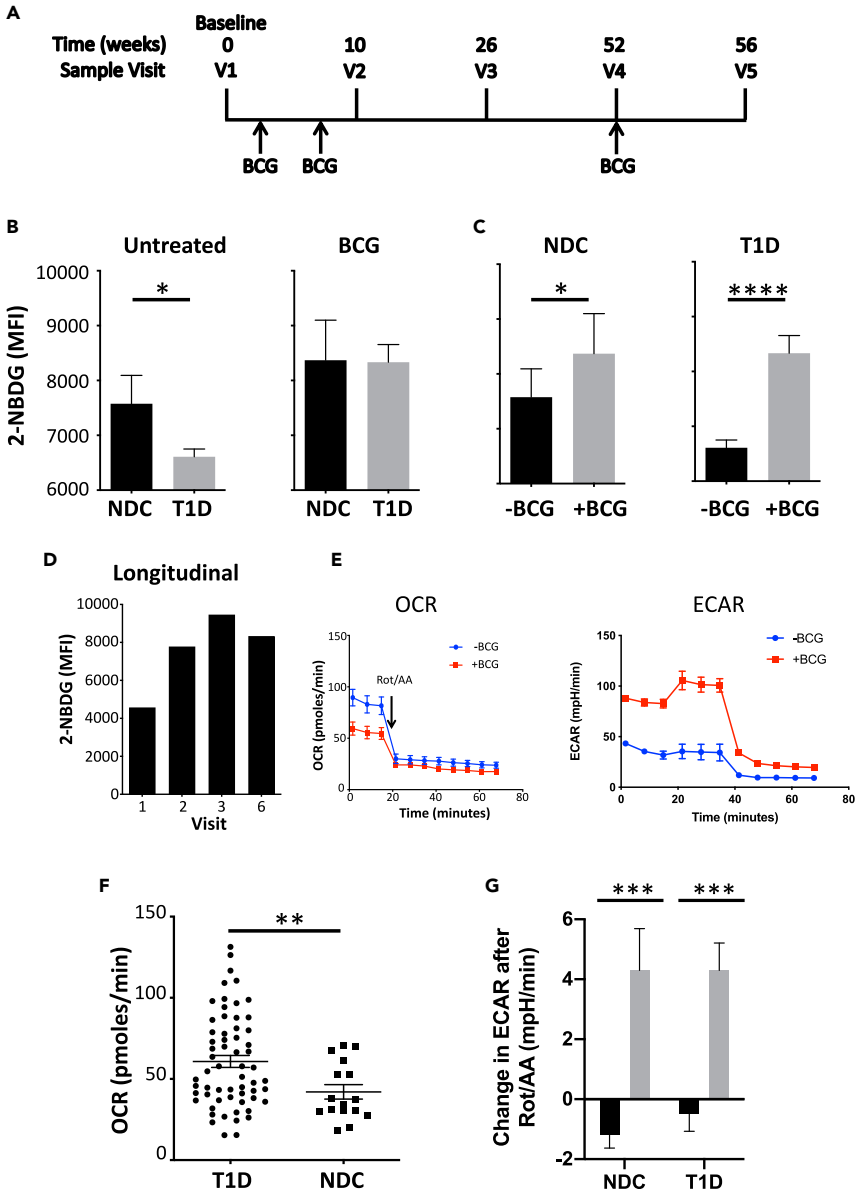

Figure 1. T1Ds Have a Baseline Defect in Aerobic Glycolysis That Is Corrected by BCG Exposure

(A)Timeline of *in vivo* BCG treatments (three vaccinations) and corresponding five serial blood samples during the 56-week-long monitoring study. The patients were treated with BCG at week 0, at week 4, and at 1 year. Blood samples were collected at serial visit times (V1–V5): V1 (0 weeks), V2 (10 weeks), V3 (26 weeks), V4 (52 weeks), and V5 (56 weeks). Total number of *in vivo* collected clinical trial blood samples (n) = 15.

(B)*In vitro* glucose uptake by untreated monocytes of T1D and nondiabetic controls (NDC) at baseline (left) compared with treatment with BCG (right). Untreated monocytes from T1Ds have poorer glucose utilization than NDC, as measured by uptake via the fluorescent glucose derivative 2-NBDG. After overnight culture, BCG increased 2-NBDG uptake in monocytes of both T1Ds (n = 21) and NDCs (n = 6) unpaired; 2-tailed t test, p = 0.02 (left), p = 0.96 (right).

(C)*In vitro* glucose uptake in monocytes of NDC (left) and T1D (right) with and without BCG exposure. Monocytes were isolated from T1D and NDC patients, cultured overnight with or without BCG, and analyzed for glucose uptake via the fluorescent glucose derivative 2-NBDG. BCG increased 2-NBDG uptake in monocytes of both T1D (n = 21) and NDC (n = 6); unpaired, 2-tailed t test, p = 0.04 (left), p < 0.0001 (right).

(D) Longitudinal *in vivo* analysis of glucose uptake by isolated monocytes harvested from a single T1D subject receiving serial BCG vaccinations (samples at V1, 2, 3, and 6). For this analysis additional samples were collected at week 78 (V6). *In vitro* glucose uptake was quantified using 2-NBDG uptake assays and showed a gradual increase over time.

Figure 1. *Continued*

(E)Representative oxygen consumption rate (OCR) and extracellular acidification rate (ECAR) assays using T1D monocytes and the Seahorse XFp analyzer. Isolated monocytes from a T1D patient were cultured for 24 h with (red) or without (blue) BCG, after which the OCR and ECAR were determined using a Seahorse XFp analyzer. At the arrow, rotenone and antimycin A (Rot/AA) were added. These reagents inhibit the electron transfer chain and as a consequence reduce OXPHOS and thus oxygen consumption as shown. BCG treatment reduces the overall oxygen consumption, indicating a switch from OXPHOS to aerobic glycolysis.

(F) Baseline OCR, a marker of OXPHOS, in monocytes of untreated T1D compared with NDC using the Seahorse XFp analyzer. The graph shows basal OCR results. Average OCR is abnormally high in T1D (n = 61) versus NDC (n = 16); unpaired t test, 2-tailed, p = 0.002.

(G) BCG increases ECAR) in cultured primary monocytes from T1D and control subjects. T1D or control monocytes were cultured with and without BCG for 7 days and analyzed using a Seahorse XFp analyzer. The increase in acidification indicates increased aerobic glycolysis after BCG treatment (total number of T1D subjects n = 42; paired t test, p = 0.0004). Level of significance in figures is indicated by asterisks: *p < 0.05; **p < 0.01; ***p < 0.001; ****p < 0.0001.

RESULTS

BCG Corrects an Underlying Defect in Glucose Utilization in T1D Monocytes

Isolated monocytes and T cells were obtained from T1D patients treated with repeat BCG vaccinations (Figure 1A). Five serial blood collections were obtained from baseline to 56 weeks after two BCG vaccines spaced four weeks apart. We also studied isolated fresh monocytes of T1D or control subjects after *in vitro* BCG exposure. Multiple methods to assess glucose utilization were employed to document the underlying defects in the utilization of glucose as the main energy source in T1D monocytes. The induction of glycolysis results in both regulated cellular glucose transport across the cell membrane and increased glucose utilization, which are of possible benefit to high glucose disease states such as diabetes. Increased glucose utilization is a result of accelerated or restored aerobic glycolysis; underactive glucose utilization can be from overactive OXPHOS (including Krebs cycle). *In vitro* cellular sugar utilization can be measured directly using the 2-NBDG assay, which measures the uptake of fluorescent deoxyglucose from the media to inside of the cell and then measured with a flow cytometer. Aerobic glycolysis is measured through the extracellular acidification rate (ECAR), whereas OXPHOS can be assessed via reduction in oxygen consumption rate (OCR), both on the Seahorse Analyzer platform.

Comparison of T1D monocytes with non-diabetic control (NDC) monocytes at baseline showed underlying defects in the uptake of 2-NBDG from the culture media, a marker of underactive aerobic glycolysis (Figure 1B, left). After a short 24-h exposure to BCG in culture, both T1D and NDC monocytes increase sugar utilization (Figure 1B, right). T1D monocytes managed to almost fully restore sugar transport as evidenced by 2-NBDG uptake that equals uptake by NDC monocytes. This suggests that T1D monocytes have the ability to augment their use of sugar and restore uptake to normal levels after BCG treatment.

We next compared baseline 2-NBDG uptake in monocytes from NDC with and without BCG treatment (Figure 1C, left). We also compared baseline 2-NBDG uptake in monocytes from TIDs with and without BCG treatment (Figure 1C, right). NDC monocytes exposed to BCG have significant increases in sugar uptake. T1D monocytes exhibit lower glucose uptake as compared with NDC monocytes at baseline but augment upward after BCG treatment.

BCG administered *in vivo* to T1D is believed to similarly utilize the lymphoid compartment to augment sugar utilization and thus lower blood sugar. Figure 1D shows the longitudinal study of one T1D patient studied for 78 weeks during three BCG vaccinations. The isolated monocytes at baseline show low glucose uptake using the 2-NBDG assay and from visit 2 to visit 6 (up to 78 weeks) show improvements in sugar utilization. Thus, BCG *in vitro* or *in vivo* can increase glucose uptake by monocytes. At baseline T1D subjects have underlying defects in the use of sugar for energy production.

BCG Treatment of Cultured T1D Monocytes Decreases Oxygen Consumption and Increases Glycolysis

We then determined the effect of BCG on cultured T1D monocytes from a single patient using the Seahorse platform. The cells were isolated from blood and analyzed in triplicate using a Seahorse Glycolytic Rate Assay (GRA assay). The basal OCR level is represented by the first three data points (the Seahorse integrates data for 3 min per data point). OXPHOS is inhibited by the addition of the electron chain inhibitors rotenone and antimycin A (Rot/AA; arrow in Figure 1E). As a result, the OCR drops and oxygen consumption is limited to nonmitochondrial processes. The convergence of the blue and red curve after Rot/AA

indicates that the differences in basal OCR are due to differences in mitochondrial oxygen consumption and not a result of differences in cell number. The OCR baseline (the first three data points) in BCG-treated monocytes is reduced compared with untreated monocytes, indicating that BCG reduces OXPHOS monitored in this assay. In a reciprocal fashion we determined the effects of BCG on cultured T1D monocytes using the ECAR assay, a measure of extracellular acidification, an indicator of augmented aerobic glycolysis. The data show the BCG induced responsiveness of these monocytes to acidify the media with BCG treatment.

T1D Monocytes Display Abnormally High Baseline Oxygen Consumption versus Nondiabetic Controls

We isolated monocytes from T1D and NDCs to compare their basal OCR after overnight culture using a Seahorse XFp external flux analyzer. Oxygen consumption is a measure of the rate of OXPHOS. Figure 1F summarizes the measurement of basal OCR by monocytes of 61 T1Ds and 16 NDCs. Average OCR is significantly higher in the T1D cohort (60.8 $\pm$ 3.7 pMoles/min) as compared with the NDC cohort (42.0 $\pm$ 4.5) (unpaired two-tailed t test, $p = 0.002$). Increased oxygen consumption indicates that T1D monocytes have increased OXPHOS as compared with NDC, suggesting that the TCA cycle in T1D is increased.

BCG Increases the Extracellular Acidification Rate in T1D and Control Monocytes

We also measured the ECAR as a result of BCG *in vitro* treatment of monocytes in T1D subjects. ECAR measures the production of acids such as lactate acid by cells, thereby serving as a measure of the amount of aerobic glycolysis. When the TCA cycle is inhibited using Rot/AA, the cells respond to the resulting deficit in ATP by increasing aerobic glycolysis. This increases the production of lactate, which increases the ECAR (Figure 1G). In monocytes cultured without BCG, there was a small reduction in ECAR after adding Rot/AA (-0.47 ± 0.60 mPH/min), whereas there was an increase in ECAR for cells cultured in the presence of BCG for 7 days (4.30 ± 0.91 mPH/min with BCG). The difference with and without BCG was significant (Figure 1G). These data indicate that BCG treatment of T1D or NDC monocytes causes an increase in aerobic glycolysis.

BCG Is Associated with Greater Myc Transcription

Myc is a "master regulator" that controls diverse cellular pathways related to glucose metabolism such as glycolysis and glutaminolysis. Figure 2A is a schematic of the central role that Myc plays in normal glucose and glutamine metabolism. According to this Myc "master regulator" model, Glut1, HK2, LDHA, and SLC1A5 are upregulated by Myc (Figure 2A; Ref 6). Glucose transporter 1 (GLUT1) is one of the transporters that facilitates the transport of glucose across the plasma membrane. HK2 phosphorylates glucose to glucose-6-phosphate. Lactate dehydrogenase (LDHA) is the key enzyme that catalyzes the conversion of pyruvate to lactate. Solute carrier family 1 member 5 (SLC1A5) is a neutral amino acid transporter that among other functions can transport glutamine across the plasma membrane.

Two other genes are under negative control by Myc. Pyruvate dehydrogenase (PDH) is the primary link between glycolysis and the TCA cycle. It catalyzes the conversion of pyruvate into acetyl CoA. Myc stimulates pyruvate dehydrogenase kinase (PDK), part of the PDH multi-enzyme complex, which in turn inhibits PDH. Thus, Myc inhibits PDH via PDK and as a result inhibits the TCA cycle. Myc also is thought to upregulate GLS, which catalyzes the hydrolysis of glutamine to glutamate. The consequence is more glutamate entering the TCA cycle, providing an alternative fuel to glucose.

We first analyzed BCG-mediated changes in transcription of Myc from *in vivo* samples of T1D treated at baseline (visit 1) and at serial BCG vaccinations (visits 2, 5). Monocytes and CD4 T cells were purified from blood of three T1D patients receiving BCG vaccinations at serial time points and Myc mRNA isolated and then analyzed using RNAseq. Figure 2B shows a comparison of RNAseq normalized reads for Myc at Visits 1, 2, and 5 (baseline, 10 weeks, 56 weeks, respectively). The Log 2 normalized reads are also presented (Figure S1). Transcription of Myc was increased in the monocytes and CD4 T cells of all T1D patients as BCG treatment progresses and was followed over the greater than one year time period.

BCG Is Associated with Increased Transcription of Myc-Controlled Genes Affecting Glucose and Glutamine Metabolism

We compared the transcription of the Myc-controlled genes in T1Ds at V1 (baseline) versus V5 (56 weeks) after the first BCG vaccination in both isolated T cells and monocytes from vaccinated human subjects.

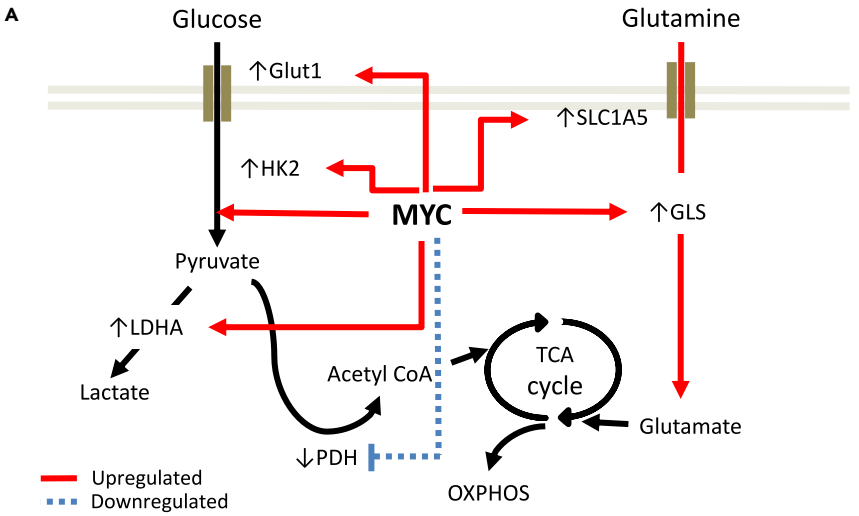

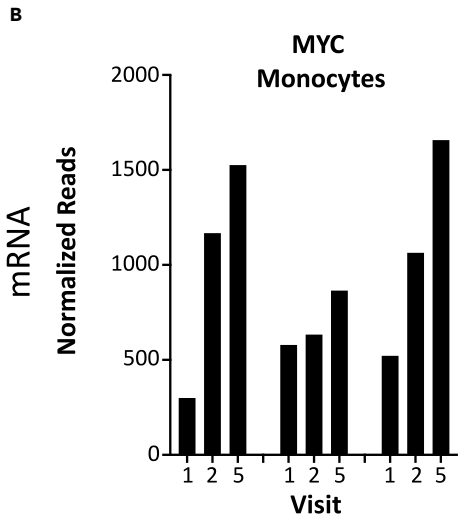

C

Normalized Reads
Monocytes

Gene	V1	V5
GLUT1	165	152
HK2	8281	8401
LDHA	13345	12990
PDHA1	1913	2064
SLC1A5	3494	3595
GLS	2296	2542

CD4 Tcells

Gene	V1	V5
GLUT1	1492	1478
HK2	816	1009
LDHA	8319	9653
PDHA1	1629	1644
SLC1A5	401	690
GLS	5111	7206

Figure 2. Induction of Myc after Repeat *in vivo* BCG Vaccinations in T1D; Restored Glycolysis and Augmented Glycolysis

(A)Schematic overview of central role of Myc and Myc-controlled pathways. The schematic shows the genes that are central to glucose and glutamine metabolism and that are under control of Myc. Gray rectangle indicates cell membrane. Red arrows indicate upregulation of gene expression by Myc. Blue dotted lines indicate downregulation by Myc. Full names of genes and their function are listed in Table S1.

(B) Myc expression, measured by mRNA, gradually increases over time in isolated monocytes from BCG-vaccinated subjects. The graph shows longitudinal data on Myc for three patients treated with BCG at baseline (V1), at 10 weeks (V2), and at 56 weeks (V5). The increase in Myc from V1 to V5 is statistically significant (1 tail, paired; $p = 0.04$, $n = 3$).

(C)Visualization of mRNA expression of Myc-controlled glycolysis and glutaminolysis genes at V1 (baseline) and V5 (56 weeks) in freshly isolated T cells and monocytes. The table shows the average normalized RNAseq data in BCG-treated T1D patients at two monitoring times. The higher numbers for each data pair are highlighted in red. For the directly controlled Myc genes (glycolysis and glutaminolysis) in both monocytes and CD4 T cells a comparison of Visit 1 (baseline prior to BCG administrations) to Visit 5 (52 weeks after two BCG vaccinations) demonstrated statistical significance of $p = 0.05$. Two genes during this monitoring interval did not respond in monocytes—GLUT1 and LDHA; one gene did not respond in CD4 T cells—GLUT1.

The results are shown in Figure 2C (higher reads are shaded in red). In monocytes, with the exception of Glut1 and LDHA, transcription of Myc-controlled genes at V5 (56 weeks) was statistically upregulated for these Myc target genes. In CD4 T cells, only Glut1 transcription was reduced while all other Myc target genes were upregulated. Therefore, overall upregulation for this Myc-controlled glycolysis pathway for both CD4 T cells and monocytes was statistically significant ($p = 0.05$).

Myc Upregulates Transcription of Genes Involved in Aerobic Glycolysis

As shown above, Myc regulates several key genes of glycolysis, and Myc is upregulated after BCG treatment of T1D monocytes and T cells. We therefore analyzed the key genes that are involved in glycolysis to determine whether these genes are also upregulated after BCG treatment. Figure 3A is a schematic overview of aerobic glycolysis and its connection to the TCA cycle as well as the alternative pathway to lactate, which is used during anaerobic conditions. The connection of glycolysis to the pentose phosphate shunt (PPP) is also shown.

The analyzed genes involved in glucose metabolism are listed in Table S1. All genes were analyzed by RNA-seq in monocytes and in CD4 T cells isolated from T1Ds receiving serial BCG vaccinations as outlined in Figure 1A. Percent changes in transcription versus baseline (V1) were calculated at V2, V4, and V5 and the results color-coded for visual comparisons. Pink and red backgrounds indicate progressive upregulation of transcription. In monocytes, changes are noticeable in V4 but become more pronounced at V5. In CD4 T cells, upregulation is already largely at a maximum at V4. The results for CD4 T cells are also shown as a bar graph in Figure 3C. At V2 many of the glucose metabolism-related genes are downregulated compared with baseline (V1), but by V4 and V5 versus baseline the great majority of these genes are upregulated. This suggests that both CD4 T cells and monocytes respond to BCG treatment *in vivo* but the time course of induction of genes may be slightly different. But both cell types increase glucose utilization through aerobic glycolysis pathways controlled by Myc.

BCG Is Associated with Increased Expression of Myc-Controlled Glutaminolysis and Polyamine Synthesis Genes

We next analyzed the effect of BCG on glutaminolysis and polyamine synthesis, two additional pathways controlled by Myc. An overview of these pathways is shown in Figure 4A. A description of the genes associated with these pathways is found in Table S1. For glutaminolysis, glutamine enters cells via transporter SLC1A5. Glutamine is then hydrolyzed to glutamate by GLS and converted to α-ketoglutarate by GLUD1, OAT1, GOT1, and GOT2. α-Ketoglutarate then enters the TCA cycle.

For polyamine synthesis, ornithine is usually produced from arginine in the urea cycle but can also be produced from glutamine. In this alternative pathway, ALDH18A1 converts glutamate into pyrroline-5-carboxylate (P-5-C), which then is turned into ornithine by OAT. Conversion of ornithine to polyamines is then performed by ODC, SRM, and SMS.

We determined the percent change in expression of these genes as compared with baseline (V1) in T1Ds treated with serial BCG vaccinations to later time points over a year later (Figure 4B). Increased expression is shown in pink and red. Decreased expression is shown in blue. Overall results show that BCG exposure is associated with a progressive and statistically significant increase in transcription of the polyamine pathway at trial start to time points of V4 (52 weeks) ($p = 0.006$) and V5 (56 weeks) ($p = 0.002$) (Figure 4B). For glutaminolysis pathway only early steps of this pathway were statistically significant such as GLS ($p = 0.02$) at both V4 (52 weeks) and V5 (56 weeks) compared with baseline but later steps in the pathway were not statistically significant.

BCG's Induction of Myc Is Associated with the HIF-1α/mTOR Pathway but Not the Akt Pathway to Promote Increased Sugar Transport

Myc and mTOR work together to increase glycolysis (Pourdehnad et al., 2013). The actions of Myc on HIF-1α- and mTOR-linked pathways are usually not related to decreased DNA methylation with increased mRNA (Figure 5A). Instead Myc regulation of this pathway can be at the level of phosphorylation or stabilization of the HIF-1α protein (Cheng et al., 2014; Doe et al., 2012). We first examined the mRNA levels of HIF-1α, mTOR, AMPK, and AKT after *in vivo* BCG treatment. As expected, we did not see a change in mRNA regulation. In past published data using PBLs and monocytes, BCG *in vitro* easily upregulated HIF-1α, in control and T1D samples (Kühtreiber, W.M. 2018). This difference is thus not due to some inherent

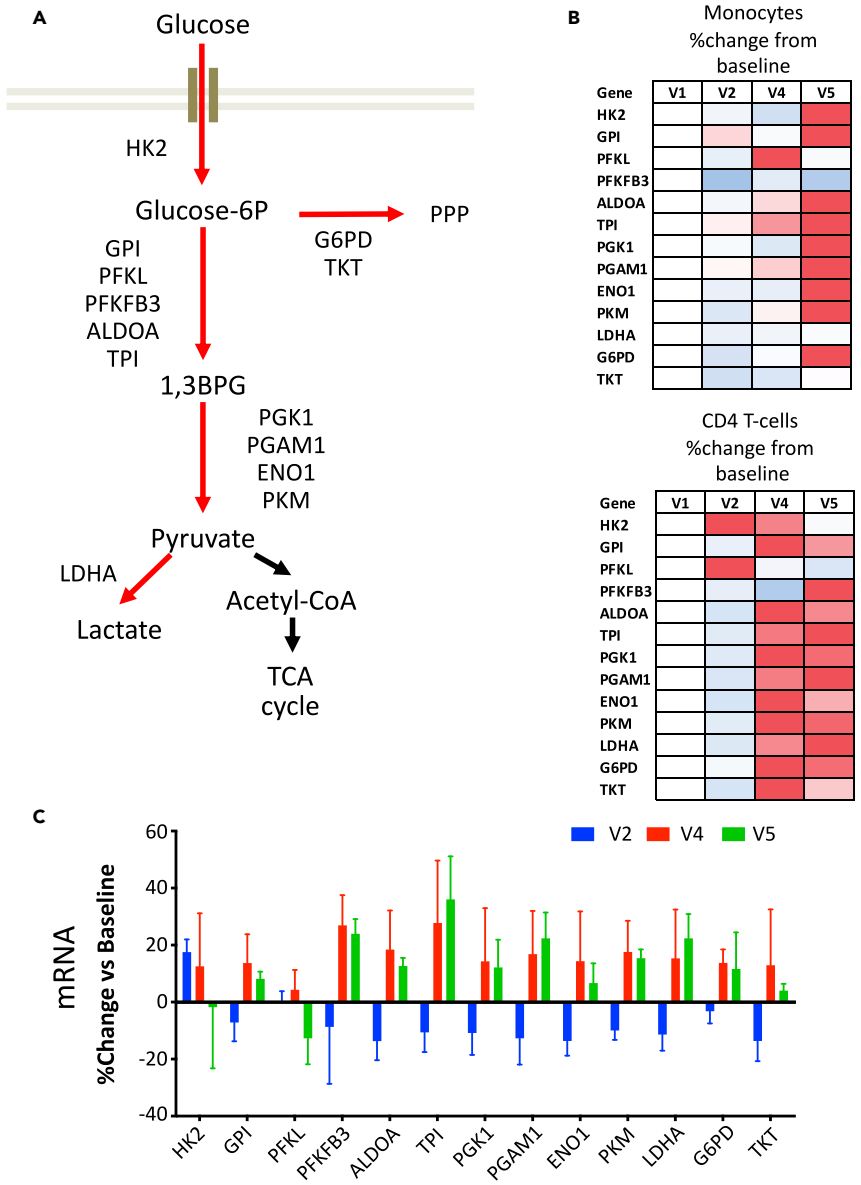

Figure 3. BCG Treatment in T1D Gradually Increases Aerobic Glycolysis and Pentose Phosphate Pathway (PPP)

(A)Schematic of glucose uptake, glycolysis and Pentose Phosphate Shunt. The data for the genes listed are shown in Figure B and C Gray rectangle indicates cell membrane. Full names of genes and their function are listed in Table S1.

(B)BCG increases the expression of many of the genes involved in glucose uptake and glycolysis in both human monocytes and CD4 T cells. The tables show the percent change of V2 (week 10), V4 (week 52), and V5 (week 56) as compared with V1 (baseline). Increases are shown in shades of red. The results show a progressive overall increase in gene expression as related to glycolysis and pentose phosphate shunt. CD4 T cells: t test V2 versus V5, p = 0.001, paired, 1-tailed, n = 3.

(C) Glycolysis- and pentose phosphate shunt-related gene expression data for CD4 T cells (n = 3, % change in gene transcription from baseline). Statistical significance values were p = 0.002, 0.80, and 0.002 for comparison of V2 versus V4; V4 versus V5; and V2 versus V5, respectively.

resistance of T1D cells to use this pathway but likely represents a timing issue with sampling extending to one year. Alternatively, *in vitro* exposures could have stronger effects.

We explored this pathway further by adding inhibitors to cultured monocytes treated for 24 h with BCG and quantifying sugar uptake into the cells using 2-NBDG flow cytometry. First, the addition of rapamycin

A

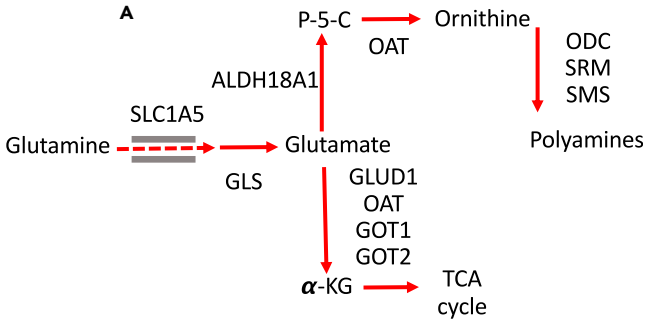

B

Glutaminolysis CD4 Tcells

	V1	V2	V4	V5
SLC1A5	0	78.6	45.8	62.4
GLS	0	32.0	12.2	29.5
OAT	0	-1.0	19.5	19.4
GLUD1	0	-15.3	4.8	-1.7
GOT1	0	5.1	17.3	28.0
GOT2	0	-4.4	11.0	12.2

Polyamine Synthesis CD4 Tcells

	V1	V2	V4	V5
ALDH18A1	0	-6.3	11.8	14.2
ODC	0	-41.0	18.5	3.3
OAT	0	-1.0	19.5	19.4
SRM	0	-13.4	24.5	13.9
SMS	0	-7.4	22.5	28.7

Figure 4. BCG Treatment Increases Glutaminolysis and Polyamine Synthesis in T1D

(A) Schematic of glutaminolysis and polyamine synthesis pathways. Expression data for the genes listed are shown in Figure 4B. Gray rectangle indicates cell membrane. Full names of genes and their function are listed in Table S1.

(B) Glutaminolysis and polyamine synthesis in CD4 T cells as compared with basal levels after *in vivo* BCG vaccinations. Shown are the up- or downregulation of transcription at visits 2 (week 10), 4 (week 52), and 5 (week 56) as compared with baseline (V1) expressed as % change. Trends are visualized by color-coding. Upregulation is highlighted in shades of red, white for no change, and blue for downregulation. The majority of genes are upregulated at V4 and V5 as compared with baseline. For polyamine synthesis there was statistically significant upregulation of all gene members occurred at baseline compared with V4 (52 weeks) ($p = 0.01$) and persisting through V5 (56 weeks) ($p < 0.00$). For glutaminolysis only the early signaling pathway was activated but later steps after glutamate were not statistically significant at this time point of 1 + years after two BCG vaccinations.

inhibited augmented glycolysis in BCG-treated monocytes (Figure 5B, left). This confirmed that BCG could augment glycolysis via mTOR. Second, inhibition of HIF-1α with ascorbate also inhibited BCG-augmented glycolysis (Figure 5B, middle). This indicated that BCG-augmented glycolysis was dependent on HIF-1α. Finally, the addition of the PI3K/AKT inhibitor, Wortmannin, to BCG-treated cells had no or minimal effect on sugar transport (Figure 5B, right). The data from these inhibition experiments support our hypothesis that BCG effects are independent of the Dectin-1 pathway and the Akt pathway. These pathways are commonly used by other microorganisms such as *Candida albicans* and work through the Dectin-1 receptor with glucan to change host cellular metabolism (Figure 5A). For BCG *in vivo* systemic effects, RNAseq analysis of CLEC7A (Dectin-1) showed that BCG is associated with gradual downregulation of this gene from *in vivo* samples (Figure S2). This also suggests that BCG works on monocytes at a different level than β-glucan to Dectin-1 (CLEC7A) receptor.

Metformin was also studied in the *in vitro* BCG-trained model of monocytes in culture (Figure S3). Metformin is a drug that activates AMPK (5′ adenosine monophosphate-activated protein kinase), an inhibitor of mTOR *in vitro* and *in vivo*. Metformin also has other targets as well. Utilizing our *in vitro* cellular sugar utilization assay (the 2-NBDG assay), T1D and control monocytes were cultured for 24 h without treatment, with BCG, with metformin, or with both. As the data in Figure S3 show in both T1D and NDC, metformin at a dose of 1 mM decreased sugar utilization; whereas, BCG, as expected, increased sugar transport. Metformin was dominant, in that the addition of metformin to BCG-treated monocytes abrogated BCG's

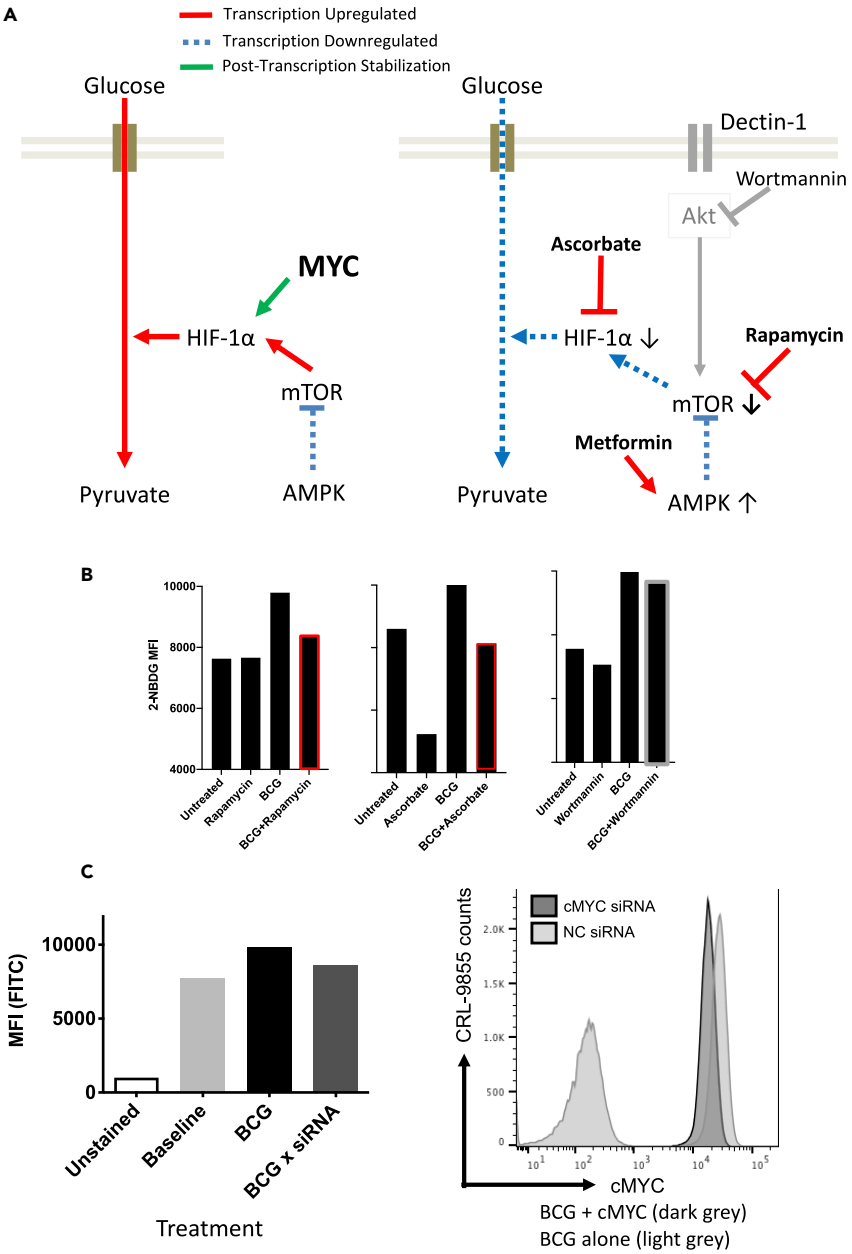

Figure 5. Confirmation of Myc Control of mTOR/HIF-1α after BCG Vaccinations, a Role in Increasing Glucose Utilization in T1D

(A) mTOR upregulates the transcription of HIF-1α, whereas Myc post-transcriptionally stabilizes HIF 1α. This allows HIF-1α to upregulate glucose uptake and aerobic glycolysis. The application of inhibitors to these pathways allowed testing of BCG's effects on this pathway. Rapamycin inhibits mTOR, which then would decrease HIF 1α levels and thus glycolysis. Ascorbate inhibits HIF 1α, and if BCG used this pathway would inhibit glycolysis. Finally if BCG's mechanism of action was similar to *Candida albicans* working through the Dectin-1 receptor then Wortmannin with BCG would inhibit Akt and decrease glycolysis.

(B) *In vitro* treatment with BCG for 24 h on monocytes with the various inhibitors helped to define the BCG dependent pathways. With the addition of rapamycin to monocytes with augmented glycolysis the accelerated glycolysis is inhibited, confirming BCG for glycolysis utilizes mTOR. Ascorbate, an inhibitor of HIF-1α, also inhibited BCG-augmented glycolysis in monocytes; BCG-augmented glycolysis was dependent on HIF-1α. Finally the addition of Wortmannin to BCG-augmented monocytes with accelerated glycolysis had no or minimal effect on sugar transport; this supports the data that BCG effects are independent of the Dectin-1 pathway and the Akt pathway.

(C) Using siRNA silencing in the CRL-9855 monocyte cell line, BCG-induced increases in glucose update are inhibited by Myc siRNA silencing treatment.

acceleration of glucose transport. Therefore, at a functional level regardless of the T1D or NDC state, Myc was exerting a level of control on this BCG-activated pathway. This was confirmed using metformin, rapamycin, and ascorbate. All three inhibited BCG-induced and Myc-accelerated sugar transport. We conclude that, at least in T1D monocytes, HIF-1α and mTOR pathways are under Myc control. These in turn assist in accelerated glycolysis as shown by glucose transport measurements.

siRNA methods were also studied to support the data in this paper on the central role of Myc in BCG-induced glucose transport in primary monocytes from T1D and NDC individuals. The siRNA method requires a cell line, because primary monocytes survive poorly with this methodology. The screening of monocyte cell lines confirmed the CRL-9855 human monocyte cell line as showing a modest increase in glucose transport when exposed *in vitro* to BCG for 3 days (Figure 5C, left). Using this cell line, we were able to show that Myc siRNA silencing inhibited augmented glucose transport (Figure 5C left). Silencing of Myc by siRNA was confirmed by comparing Myc levels in cells that were transfected with Myc siRNA versus cells that were transfected with negative control siRNA. Flow cytometry showed that Myc was substantially downregulated in the cells treated with Myc siRNA as compared with the negative controls (Figure 5C, right). This thus confirmed the functional association between Myc control and BCG-accelerated glucose transport in monocytes.

DISCUSSION

Metabolic pathways are altered after immune cells become activated or stimulated with live microorganisms, a process called immunometabolism (Pearce and Pearce, 2013). As the fine details of immunometabolism become worked out in various test host microbe systems, often *in vitro*, the metabolic changes can be correlated to the type of external cellular stimulus (Kelly and O'Neill, 2015; Everts et al., 2014, Krawczyd et al, 2010, Rodríguez-Prados et al., 2010). Commonly the end result is increased glycolytic rates and induction of pathways for enhanced sugar utilization with minimized reliance on the Krebs cycle. Indeed this is what we find in the present year-long human study of *in vivo* BCG vaccination in the setting of T1D.

We have shown here that T1D lymphoid cells display an underlying baseline defect in aerobic glycolysis, perhaps due to inadequate microbial exposures. This explanation is consistent with the hygiene hypothesis (Strachan, 1989). After either *in vitro* or *in vivo* BCG exposure, we observe the gradual correction and improvement of aerobic glycolysis toward normal levels. We profiled the *in vivo* immune cell metabolism in T1D subjects and focused on the metabolic pathways that require Myc involvement. Here we demonstrated the gradual year-long elevation in Myc mRNA after BCG vaccinations that appears to affect all known pathways regulated by Myc. The data consistently show the gradual *in vivo* induction by Myc of the glycolysis pathways, in both T cells and monocytes in vaccinated humans with T1D. Furthermore, we found that BCG stimulates glutamine utilization while in parallel stimulating the mRNA proteins of glutaminolysis. Polyamine synthesis is also gradually induced in BCG-treated cohorts. Finally, Myc control of HIF-1α/mTOR augments glycolysis, whereas inhibition with metformin, rapamycin, and ascorbate confirm a close connection to three Myc pathways for lowering blood sugars. The data pull together many of the sugar regulation pathways under Myc's regulatory control: glycolysis, glutaminolysis, polyamine synthesis, and the HIF-1α/mTOR pathway (Goetzman and Prochownik, 2018; Rathmell, 2011; Wang et al., 2011).

Innate immunity from host microbe interactions is recognized to change immune system metabolism. Glycolytic reprogramming has been described related to the TLR ligands, and mycobacteria use these receptors (Krawczyk et al., 2010). The levels of host-microbe control for mycobacteria, including the attenuated *Mycobacterium bovis* of the BCG vaccine include changes in DNA methylation, changes in mRNA splice forms, changes in the phosphorylation patterns of proteins, changes in mRNA levels, and even protein to protein stability. Multiple confirmatory studies show that microbes including BCG can at the DNA level alter gene methylation patterns, a process now often termed "trained immunity" (Netea et al., 2016). BCG as well as its pathogenic version, tuberculosis, are known to also exert host control by changing protein phosphorylation patterns, often with increasing cAMP levels from a multitude of mycobacterial genes devoted to this process inflicted on the host (Bai et al., 2011). Infection with *Mycobacterium tuberculosis* induces aerobic glycolysis in human alveolar macrophages (Gleeson and Sheedy, 2016). BCG both *in vitro* and *in vitro* induces a strong increase in glycolysis and also glutamine metabolism (Arts et al., 2016). Not all infections may use the same host metabolic pathways with viruses and bacteria pursuing varying course as it relates to glucose. Glucose utilization was required for survival in animal models of viral inflammation but for bacterial infections ketogenesis was required (Wang et al., 2016). For the *B*-glucan

component of *Candida albicans*, the host interaction is through the surface Dectin-1 receptor and the intracellular Akt pathway (Cheng S.C. et al., 2014). The presented data show the BCG organism does not use the Akt pathway to augment host aerobic glycolysis.

Myc itself, in the present study, is shown to exert its effects at the mRNA transcription level, but ultimately its effect on the HIF-1α/mTOR pathway has previously been demonstrated to be at the phosphorylation-dependent and protein stability level. This powerful host-microbe level of control is exceptional because there are at least 15 distinct adenyl cyclases, the protein that generates cAMP in the genomes of *Mycobacterium tuberculosis* and also similar cAMP genes in *Mycobacterium bovis* for the BCG vaccine. Myc also regulates glycolytic genes by preferentially switching the expression of PKM1 to PKM2 by alternative splicing of the transcript (Dang and Semenza, 1999; David et al., 2010). With so many molecular levels for microbes to control host responses, in this study we reverted to direct sugar transport assays as an endpoint for the host microbe outcome, such as to verify the Myc signaling control on HIF-1α/mTOR pathway.

There is still much unknown about the effects of BCG on *in vivo* cellular metabolism. The present study of humans with T1D extended over a year of 5–6 serial blood sample collections and three BCG vaccinations for over one-year time period. Future studies will be aimed at following patients for 5 years. Two such studies are underway. A human study by Matsumiya and colleagues showed BCG by 7–14 days as having effects on glycolysis pathways, although the study did not identify specific genes or pathway steps (Matsumiya et al., 2015). A three-month study of normal humans vaccinated with one BCG dose saw control of epigenetics with effects on histone markers (H3K4me3 and H3K9me3) (Arts R, 2016). Earlier *in vitro* studies found epigenetic modifications at the chromatin level after BCG exposure (Kleinnijenhuis et al., 2012). It is recognized that diverse environmental challenges from microbes can alter epigenetic patterns especially those involving interactions between histones and effector proteins (Busslinger and Tarakhovsky, 2014). Published studies show that the epigenetic effects of BCG that are related to the immune system lead to the desired *in vivo* expansion and activation of beneficial immune cells such as Tregs, formerly known as T suppressor cells. BCG vaccinations in T1D subjects demonstrated both mRNA and corresponding statistically significant epigenetic changes to many CG sites in six Treg signature genes—Foxp3, TNFRSF18, IL2RA, IKZF2, IKZF4, and CTLA4. These epigenetic changes could be observed as early as eight weeks after the first BCG vaccine (Kühtreiber et al., 2018). We are now studying gene methylation patterns as a mechanism for how an infection by BCG can have such long lasting metabolic effects on glucose regulation. In addition, we will look for effects at the level of phosphorylation and protein activation or other modes of interactions of host and microbes, such as the role of Myc in stabilizing the HIF-1α protein for prolonged function (Doe et al., 2012).

It is known that many of the clinical effects of BCG vaccinations in humans are delayed by months and years after vaccine administration but effects can persist for decades. Indeed, in the present study we chart a time course of at least a year during which there is a gradual upregulation of Myc at the mRNA level, and this is accompanied by fresh human T1D monocyte samples gradually obtaining restored sugar transport. In our Phase 1 clinical trial in adults with >15 years of disease it took up to 3 years after BCG administration to reach almost complete correction of blood sugars as measured by HbA1c. Children with T1D may respond faster but this has not yet been formally tested in double-blinded clinical trials. Also, a multiple sclerosis clinical trial using BCG vaccines found a similar 2-year delay prior to observing clinical improvement (Ristori et al., 1999). This stresses that the basic science of host-microbe interactions need to be studied in long studies with longitudinal sampling. This is the first long-term longitudinal data on this host microbe interaction at the molecular level for Myc gene regulation in the diabetic host. It has been speculated that the reason for the delay in significant clinical effects is because the vaccine is administered intradermally. In animal models, if BCG is administered IV, thus resulting in bone marrow chimerism and re-programming of bone marrow stem cells, the effects are dramatically expedited (Das et al., 2013; Kaufmann et al., 2018). BCG resetting of the bone marrow may also account for why the durability of this host-microbe interaction is so long lasting, not only in BCG-treated T1D but also in phase II clinical trials of BCG in multiple sclerosis. Similar to T1D, multiple sclerosis patients have a baseline impairment in glycolysis, and some studies suggest that the earliest CNS brain lesions first show aerobic glycolysis defects (La Rocca et al., 2017). Therefore, defective aerobic glycolysis may be a common feature of the lymphoid dysfunction in human autoimmune subjects, as well as these same defects perhaps also expressing in target tissue.

T1D has a propensity for bacterial infections, thus resulting in skin infections, styes, gangrene of the legs, urinary tract infections, and more (Abu-Ashour et al., 2018). Metabolic requirements including ambient

glucose during infection vary with the etiology of the infections. For instance, bacterial infections often improve with normal glucose levels and bacterial infections progress with high glucose levels in feeding states (Wang et al., 2016). Therefore, BCG vaccinations might ultimately decrease bacterial infections in T1D. The current study is too small and too short of duration (just over a year) but further longer studies with BCG vaccinations in T1D up to 5 years have been designed to qualify and tract infectious disease consequences after BCG vaccinations.

Does the improved blood glucose control seen in type 1 diabetes have any applicability to type 2 diabetes? Although some animal data support this premise, there is also human data. A 60-year follow-up study of the long-term efficacy of the BCG vaccine in American Indians and Alaska Natives has shown not only protection from tuberculosis and protection from lung cancer but also a statistically significant lowering of type 2 diabetes incidence (Aronson et al., 2019; Usher et al., 2019; van Dam et al., 2016; Inafuku et al., 2015).

The goal in immune metabolism is to attain the right balance—not too much of a good thing. Indeed BCG almost restores glucose metabolism to near normal as measured by mRNA expression, at least in monocytes and T cells, and also improves monocyte glucose transport to near normal in typical early onset type 1 diabetic subjects. It is not the overcorrection of glucose metabolism to pathologic states (such as the Warburg effect) that is desired. BCG's correction of a glucose utilization defect by Myc cellular mechanisms is a tightly controlled process preventing hypoglycemia, unlike delivery of a protein such as insulin that lowers blood sugars in unregulated ways. In sum, we have shown here that BCG induces Myc transcription and heightens transcription of most Myc glucose-regulating target genes in the four pathways depicted here. Taken together, the data suggest a beneficial host-microbe interaction that delivers a systemic correction of a lymphoid sugar utilization defect in T1D.

Limitations of the Study

The limitations of this study include the use of BCG in type 1 diabetic subjects with long-standing type 1 diabetes; pediatric trials have not yet been conducted to understand the kinetics of blood sugar corrections and the central signaling pathways in younger subject with BCG vaccination treatment. The speed of glucose utilization recovery may also be different in younger subjects.

In adult humans we can easily measure glucose utilization and the role of Myc in T cells and monocytes derived from peripheral blood. Although the lymphoid system is the second largest cellular organ in the human, we do not yet know if BCG could also be working at the level of glucose utilization in other organs such as the liver, muscle, or the kidneys. For human studies we cannot sample human liver, brain, etc. to see if those changes are also occurring in response to BCG. An ongoing 5-year-long study with FDG-PET scan imaging of organ system for utilization of sugar after BCG with FDG-PET scan imaging should help to answer these questions in the future.

The cellular volume of the lymphoid system is frequently underestimated so its' capacity to use sugar and regulated sugar transport is underappreciated. Using cell numbers alone, the lymphoid system is the largest human organ. Remember the human lymphoid system is composed of blood (RBC, WBC, platelets, neutrophils, monocytes, eosinophils, etc.), lymph nodes, spleen, bone marrow, lymph system, thymus etc. For an average human body it is composed of 1.12 × 10^13 lymphoid cells. The total body cell number is 3.7 × 10^13 cells. This compares to liver with 2.31 × 10^11 cells, compares to muscle with 2.50 × 10^8 cells, brain 1 × 10^11 cells (Bianconi et al., 2013; Harrison, 1962). Using cell numbers the lymphoid system dwarfs the liver, brain, and muscle combined in total cellular numbers that could utilize sugar more efficiently with restored normal levels of aerobic glycolysis. It is feasible the lymphoid system alone corrects this defect but human data on other organ systems will gradually accumulate. These subjects are not off insulin but use reduced insulin and their HbA1c drop to the near normal range without hypoglycemia.

Lastly very rare inborn errors of metabolism in aerobic glycolysis in lymphocytes are associated in some cases with ketosis-prone insulin-dependent diabetes suggesting but not proving the novel role of the lymphoid system contributing to regulated sugar levels (Afadhel and Babiker, 2018).

METHODS

All methods can be found in the accompanying Transparent Methods supplemental file.

SUPPLEMENTAL INFORMATION

Supplemental Information can be found online at https://doi.org/10.1016/j.isci.2020.101085.

ACKNOWLEDGMENTS

We thank Dr Miriam Davis for a critical read of the manuscript and The Iacocca Foundation for their financial support.

AUTHOR CONTRIBUTIONS

Conducting experiments: WK, RK, YS, LT, TL, SS, LM, JG, GS, HT. Conceptual input, design, statistical analysis, and supervision: WK, DF.

DECLARATION OF INTERESTS

The authors declare no competing interests.

Received: January 26, 2020
Revised: April 3, 2020
Accepted: April 15, 2020
Published: May 22, 2020

REFERENCES

Abu-Ashour, W., Twells, L.K., Valcour, J.E., and Gamble, J.M. (2018). Diabetes and the occurrence of infection in primary care: matched cohort study. BMC Infect. Dis. *18*, 67–70.

Afadhel, M., and Babiker. (2018). A. Inborn errors of metabolism associated with hyperglycemic ketoacidosis and diabetes mellitus; narrative review. Sudan J. Pediatr. *18*, 10–23.

Airaghi, L., and Tedeschi, A. (2006). Negative association between occurrence of type 1 diabetes and tuberculosis incidence at population level. Acta Diabetol. *43*, 43–45.

Andersen, E., Isager, H., and Hyllested, K. (1981). Risk factors in multiple sclerosis: Tuberculin reactivity, age at measles infection, tonsillectomy and appendectomy. Acta Neurol. Scand. *63*, 131–135.

Aronson, N.E., Santosham, M., Comstock, G.W., Howard, R.S., Moulton, L.H., Rhoades, E.R., and Harrison, L.H. (2019). Long-term efficacy of BCG vaccine in American Indians and Alaska natives - a 60-year follow-up study. JAMA *291*, 1086–2091.

Arts, R.J.W., Varvalho, A., LaRocca, C., et al. (2016). Immunometabolic pathways in BCG-induced trained immunity. Cell Rep. *17*, 2562–2571.

Bach, J.-F. (2002). The effect of infections on susceptibility to autoimmune and allergic diseases. N. Engl. J. Med. *347*, 911–920.

Bai, G., Knapp, G.S., and McDonough, K.A. (2011). Cyclic AMP signalling in mycobacteria: redirecting the conversation with a common currency. Cell. Microbiol. *13*, 349–358.

Bianconi, E., Piovessan, A., Facchin, F., et al. (2013). An estimation of the number of cells in the human body. Ann. Hum. Biol. *40*, 471–481.

Bloomfield, S.F., Rook, G.A., Scott, E.A., Shanahan, F., Stanwell-Smith, R., and Turner, P. (2016). Time to abandon the hygiene hypothesis: new perspectives on allergic disease, the human microbiome, infectious disease prevention and the role of targeted hygiene. Perspect. Public Health *136*, 213–224.

Brites, D., and Gagneux, S. (2015). Co-evolution of Mycobacterium tuberculosis and Homo sapiens. Immunol. Rev. *264*, 6–24.

Busslinger, M., and Tarakhovsky, A. (2014). Epigenetic control of immunity. Cold Spring Harb. Perspect. Biol. *6*, a019307.

Cheng, S.-C., Quintin, J., Cramer, R.A., Shepardson, K.M., Saeed, S., Kumar, V., Giamarellos-Bourboulis, E.J., Martens, J.H.A., Rao, N.A., Aghajanirefah, A., et al. (2014). mTOR/HIF1α-mediated aerobic glycolysis as metabolic basis for trained immunity. Science *345*, 1250684.

van Dam, A.D., Bekkering, S., Crasborn, M., et al. (2016). BCG lowers plasma cholesterol levels and delays atherosclerotic lesion progression in mice. Atherosclerosis *251*, 6–14.

Dang, C.V., and Semenza, G.L. (1999). Oncogenic alterations of metabolism. Trends Biochem. Sci. *24*, 68–72.

Dang, C.V., O'Donnell, K.A., Zeller, K.I., Nguyen, T., Osthus, R.C., and Li, F. (2006). The c-Myc target gene network. Semin. Cancer Biol. *16*, 253–264.

Dang, C.V., Le, A., and Gao, P. (2009). MYC-induced cancer cell energy metabolism and therapeutic opportunities. Clin. Cancer Res. *15*, 6479–6483.

Das, B., Kashino, S.S., Pulu, I., Kalita, D., Swami, V., Yeger, H., Felsher, D.W., and Campos-Neto, A. (2013). CD271(+) bone marrow mesenchymal stem cells may provide a niche for dormant Mycobacterium tuberculosis. Sci. Transl Med. *5*, 170ra13.

David, C.J., Chen, M., Assanah, M., Canoll, P., and Manley, J.L. (2010). HnRNP proteins controlled by c-Myc deregulate pyruvate kinase mRNA splicing in cancer. Nature *463*, 364–368.

Doe, M.R., Ascano, J.M., Kaur, M., and Cole, M.D. (2012). Myc posttranscriptionally induces HIF1 protein and target gene expression in normal and cancer cells. Cancer Res. *72*, 949–957.

Everts, B., Amiel, E., Huang, S.C.-C., Smith, A.M., Chang, C.-H., Lam, W.Y., Redmann, V., Freitas, T.C., Blagih, J., van der Windt, G.J.W., et al. (2014). TLR-driven early glycolytic reprogramming via the kinases TBK1-IKKε supports the anabolic demands of dendritic cell activation. Nat. Immunol. *15*, 323–332.

Faustman, D.L., Wang, L., Okubo, Y., Burger, D., Ban, L., Man, G., Zheng, H., Schoenfeld, D., Pompei, R., Avruch, J., et al. (2012). Proof-of-Concept, randomized, controlled clinical trial of Bacillus-Calmette-Guerin for treatment of long-term type 1 diabetes. PLoS One *7*, e41756.

Gleeson, L.E., Sheedy, F.J., et al. (2016). Cutting Edge: Mycobacterium tuberculosis induces aerobic glycolysis in human alveolar macrophages that is required for control of intracellular bacillary replication. J. Immunol. *15*, 2444–2449.

Goetzman, E.S., and Prochownik, E.V. (2018). The role for Myc in coordinating glycolysis, oxidative phosphorylation, glutaminolysis, and fatty acid metabolism in normal and neoplastic tissues. Front. Endocrinol. (Lausanne) *9*, 129.

Guo, Q.M., Malek, R.L., Kim, S., Chiao, C., He, M., Ruffy, M., Sanka, K., Lee, N.H., Dang, C.V., and Liu, E.T. (2000). Identification of c-Myc responsive genes using rat cDNA microarray. Cancer Res. *60*, 5922–5928.

Harrison, W.J. (1962). The total cellularity of the bone marrow in man. J. Clin. Pathol. *15*, 254–259.

Inafuku, M., Matcuzaki, G., and Oku, H. (2015). Intravenous Mycobacterium Bovis Bacillus Calmett-Guerin ameliorates nonalcoholic fatty

liver disease in obese, diabetic ob/ob mice. PLoS One. https://doi.org/10.1371/journal.pone.0128676.

Kaufmann, E., Sanz, J., Dunn, J.L., Khan, N., Mendonça, L.E., Pacis, A., Tzelepis, F., Pernet, E., Dumaine, A., Grenier, J.-C., et al. (2018). BCG educates hematopoietic stem cells to generate protective innate immunity against. Tuberculosis. Cell *172*, 176–190.e19.

Kelly, B., and O'Neill, L.A.J. (2015). Metabolic reprogramming in macrophages and dendritic cells in innate immunity. Cell Res *25*, 771–784.

Kim, J., and Dang, C.V. (2006). Cancer's molecular sweet tooth and the Warburg effect. Cancer Res. *66*, 8927–8930.

Kleinnijenhuis, J., Quintin, J., Preijers, F., Joosten, L.A.B., Ifrim, D.C., Saeed, S., Jacobs, C., van Loenhout, J., de Jong, D., Stunnenberg, H.G., et al. (2012). Bacille Calmette-Guérin induces NOD2-dependent nonspecific protection from reinfection via epigenetic reprogramming of monocytes. Proc. Natl. Acad. Sci. U S A *109*, 17537–17542.

Kodaman, N., Sobota, R.S., Mera, R., Schneider, B.G., and Williams, S.M. (2014). Disrupted human-pathogen co-evolution: a model for disease. Front. Genet. *5*, 290.

Kondrashova, A., Reunanen, A., Romanov, A., Karvonen, A., Viskari, H., Vesikari, T., Ilonen, J., Knip, M., and Hyöty, H. (2005). A six-fold gradient in the incidence of type 1 diabetes at the eastern border of Finland. Ann. Med. *37*, 67–72.

Krawczyk, C.M., Holowka, T., Sun, J., Blagih, J., Amiel, E., DeBerardinis, R.J., Cross, J.R., Jung, E., Thompson, C.B., Jones, R.G., et al. (2010). Toll-like receptor-induced changes in glycolytic metabolism regulate dendritic cell activation. Blood *115*, 4742–4749.

Kühtreiber, W.M., and Faustman, D.L. (2019). BCG Therapy for type 1 diabetes: restoration of balanced immunity and metabolism. Trends Endocrinol. Metab. *30*, 80–92.

Kühtreiber, W.M., Tran, L., Kim, T., Dybala, M., Nguyen, B., Plager, S., Huang, D., Janes, S., Defusco, A., Baum, D., et al. (2018). Long-term reduction in hyperglycemia in advanced type 1 diabetes: the value of induced aerobic glycolysis with BCG vaccinations. NPJ Vaccin. *3*, 1–14.

Lachmandas, E., Boutens, L., Ratter, J.M., Hijmans, A., Hooiveld, G.J., Joosten, L.A.B., Rodenburg, R.J., Fransen, J.A.M., Houtkooper, R.H., van Crevel, R., et al. (2016). Microbial stimulation of different Toll-like receptor signalling pathways induces diverse metabolic programmes in human monocytes. Nat. Microbiol. *2*, 16246.

Le, A., Lane, A.N., Hamaker, M., Bose, S., Gouw, A., Barbi, J., Tsukamoto, T., Rojas, C.J., Slusher, B.S., Zhang, H., et al. (2012). Glucose-independent glutamine metabolism via TCA cycling for proliferation and survival in B-cells. Cell Metab. *15*, 110–121.

Lewis, B.C., Shim, H., Li, Q., Wu, C.S., Lee, L.A., Maity, A., and Dang, C.V. (1997). Identification of putative c-Myc-responsive genes: characterization of rcl, a novel growth-related gene. Mol.Cell Biol. *17*, 4967–4978.

Matsumiya, M., Satti, I., Chomka, A., Harris, S.A., Stockdale, L., Meyer, J., Fletcher, H.A., and McShane, H. (2015). Gene expression and cytokine profile correlate with mycobacterial growth in a human BCG challenge model. J.Infect. Dis. *211*, 1499–1509.

Netea, M.G., Joosten, L.A.B., Latz, E., Mills, K.H.G., Natoli, G., Stunnenberg, H.G., O'Neill, L.A.J., and Xavier, R.J. (2016). Trained immunity: a program of innate immune memory in health and disease. Science *352*, aaf1098.

Nilsson, J.A., Keller, U.B., Baudino, T.A., Yang, C., Norton, S., Old, J.A., Nilsson, L.M., Neale, G., Kramer, D.L., Porter, C.W., et al. (2005). Targeting ornithine decarboxylase in Myc-induced lymphomagenesis prevents tumor formation. Cancer Cell *7*, 433–444.

Osthus, R.C., Shim, H., Kim, S., Li, Q., Reddy, R., Mukherjee, M., Xu, Y., Wonsey, D., Lee, L.A., and Dang, C.V. (2000). Deregulation of glucose transporter 1 and glycolytic gene expression by c-Myc. J. Biol. Chem. *275*, 21797–21800.

Palsson-McDermott, E.M., Curtis, A.M., Goel, G., Lauterbach, M.A.R., Sheedy, F.J., Gleeson, L.E., van den Bosch, M.W.M., Quinn, S.R., Domingo-Fernandez, R., Johnston, D.G.W., et al. (2015). Pyruvate kinase M2 regulates Hif-1α activity and IL-1β induction and is a critical determinant of the warburg effect in LPS-activated macrophages. Cell Metab. *21*, 65–80.

Pearce, E.L., and Pearce, E.J. (2013). Metabolic pathways in immune cell activation and quiescence. Immunity *18*, 633–643.

Pourdehnad, M., Truitt, M.L., Siddiqi, I.N., Ducker, G.S., Shokat, K.M., and Ruggero, D. (2013). Myc and mTOR converge on a common node in protein synthesis control that confers synthetic lethality in Myc-driven cancers. Proc. Natl. Acad. Sci. U S A *110*, 11988–11993.

Ramanathan, A., Wang, C., and Schreiber, S.L. (2005). Perturbational profiling of a cell-line model of tumorigenesis by using metabolic measurements. Proc. Natl. Acad. Sci. U S A *102*, 5992–5997.

Rathmell, J.C. (2011). T cell Myc-tabolism. Immunity *35*, 845–846.

Ristori, G., Buzzi, M.G., Sabatini, U., Giugni, E., Bastianello, S., Viselli, F., Buttinelli, C., Ruggieri, S., Colonnese, C., Pozzilli, C., et al. (1999). Use of Bacille Calmette-Guèrin (BCG) in multiple sclerosis. Neurology *53*, 1588–1589.

La Rocca, C., Carbone, F., De Rosa, V., Colamatteo, A., Galgani, M., Perna, F., Lanzillo, R., Brescia Morra, V., Orefice, G., Cerillo, I., et al. (2017). Immunometabolic profiling of T cells from patients with relapsing-remitting multiple sclerosis reveals an impairment in glycolysis and mitochondrial respiration. Metab. Clin. Exp. *77*, 39–46.

Rodríguez-Prados, J.-C., Través, P.G., Cuenca, J., Rico, D., Aragonés, J., Martín-Sanz, P., Cascante, M., and Boscá, L. (2010). Substrate fate in activated macrophages: a comparison between innate, classic, and alternative activation. J. Immunol. *185*, 605–614.

Ruiz-García, A., Monsalve, E., Novellasdemunt, L., Navarro-Sabaté, A., Manzano, A., Rivero, S., Castrillo, A., Casado, M., Laborda, J., Bartrons, R., et al. (2011). Cooperation of adenosine with macrophage Toll-4 receptor agonists leads to increased glycolytic flux through the enhanced expression of PFKFB3 gene. J. Biol. Chem. *286*, 19247–19258.

Shi, L., Salamon, H., Eugenin, E.A., Pine, R., Cooper, A., and Gennaro, M.L. (2015). Infection with Mycobacterium tuberculosis induces the Warburg effect in mouse lungs. Sci. Rep. *5*, 18176.

Shim, H., Dolde, C., Lewis, B.C., Wu, C.-S., Dang, G., Jungmann, R.A., Dalla-Favera, R., and Dang, C.V. (1997). c-Myc transactivation of LDH-A: implications for tumor metabolism and growth. Proc. Natl. Acad. Sci. U S A *94*, 6658–6663.

Stienstra, R., Netea-Maier, R.T., Riksen, N.P., Joosten, L.A.B., and Netea, M.G. (2017). Specific and complex reprogramming of cellular metabolism in myeloid cells during innate immune responses. Cell Metab. *26*, 142–156.

Strachan, D.P. (1989). Hay fever, hygiene, and household size. BMJ *299*, 1259–1260.

Tan, Y., Zanoni, I., Cullen, T.W., Goodman, A.L., and Kagan, J.C. (2015). Mechanisms of Toll-like receptor 4 endocytosis reveal a common immune-evasion strategy used by pathogenic and commensal bacteria. Immunity *43*, 909–922.

Usher, N.T., Chang, S., Howard, R.S., Martinez, A., Harrison, L.H., Santosham, M., and Aronson, N.E. (2019). Association of BCG vaccination in childhood with subsequent cancer diagnoses; a 60-year follow-up of a clinical trial. JAMA Open Netw. *2*, e1912014.

Wang, A., Huen, S.C., Luan, H.H., Yu, S., Zhang, C., Gallezot, J.D., Booth, C.J., and Medzhitov, R. (2016). Opposing effects of fasting metabolism on tissue tolerance in bacterial and viral inflammation. Cell *166*, 1512–1525.

Wang, R., Dillon, C.P., Shi, L.Z., Milasta, S., Carter, R., Finkelstein, D., McCormick, L.L., Fitzgerald, P., Chi, H., Munger, J., et al. (2011). The transcription factor Myc controls metabolic reprogramming upon T lymphocyte activation. Immunity *35*, 871–882.

iScience, Volume *23*

Supplemental Information

BCG Vaccinations Upregulate Myc, a Central Switch for Improved Glucose Metabolism in Diabetes

Willem M. Kühtreiber, Hiroyuki Takahashi, Ryan C. Keefe, Yaerin Song, Lisa Tran, Trevor G. Luck, Gabriella Shpilsky, Louisa Moore, Sarah M. Sinton, Jessica C. Graham, and Denise L. Faustman

Supplemental Table 1. Metabolism genes discussed in this paper

Symbol	Name	**Description** (See Ref 13)
Glucose Metabolism		
HK2	Hexokinase 2	Phosphorylates Glucose to Glucose-6P and is known to be a rate-controlling step in glucose metabolism
GPI	Glucose-6-Phosphate Isomerase	Interconverts glucose-6-phosphate and fructose-6-phosphate
PFKL	Phosphofructokinase, Liver Type	Catalyzes the conversion of D-fructose 6-phosphate to D-fructose 1,6-biphosphate
PFKFB3	6-Phosphofructo-2-Kinase/ Fructose-2,6-Biphosphatase 3	Involved in both synthesis and degradation of fructose-2,6-bisphosphate
ALDOA	Aldolase, Fructose-Bisphosphate A	Catalyzes the reversible conversion of fructose-1,6-bisphosphate to glyceraldehyde 3-phosphate and dihydroxyacetone phosphate
TPI	Triose-Phosphate Isomerase	Catalyzes the isomerization of glyceraldehydes 3-phosphate and dihydroxy-acetone phosphate
PGK1	Phosphoglycerate Kinase 1	Catalyzes the conversion of 1,3-diphosphoglycerate to 3-phosphoglycerate
PGAM1	Phosphoglycerate Mutase 1	Catalyzes the reversible reaction of 3-phosphoglycerate (3-PGA) to 2-phosphoglycerate (2-PGA) in the glycolytic pathway
ENO1	Enolase 1, α-Enolase	Catalyzes the conversion of 2-phosphoglycerate to phosphoenolpyruvate
PKM	Pyruvate Kinase M1/2	Catalyzes the transfer of a phosphoryl group from phosphoenolpyruvate to ADP, generating ATP and pyruvate
LDHA	Lactate Dehydrogenase A	Catalyzes the conversion of L-lactate and NAD to pyruvate and NADH
G6PD	Glucose-6-Phosphate Dehydrogenase	Converts D-glucose 6-phosphate into glucono-1,5-lactone
TKT	Transketolase	Plays a role in the channeling of excess sugar phosphates to glycolysis in the pentose phosphate pathway
MYC	(cMYC) Cellular Myelocytomatosis Proto Oncogene	Plays a pivotal role in metabolic reprogramming of cells by enhancing glycolysis, lactate production, glutaminolysis and oxidative phosphorylation.
mTOR	Mechanistic (Mammalian) Target of Rapamycin	Protein kinase that directly or indirectly regulates the phosphorylation of many proteins
Glutaminolysis		
SLC1A5	Solute Carrier Family 1 Member 5	Amino acid transporter that transports glutamine into cells
GLS2	Glutaminase 2	Catalyzes the hydrolysis of glutamine to glutamate and ammonia
GLUD1	Glutamate Dehydrogenase 1	Converts glutamate into $\boldsymbol{\alpha}$-ketoglutarate
OAT	Ornithine Aminotransferase	Converts glutamate into $\boldsymbol{\alpha}$-ketoglutarate
GOT1, GOT2	Glutamic- Oxaloacetic Transaminase 1, 2	Converts glutamate into $\boldsymbol{\alpha}$-ketoglutarate
Polyamine Synthesis		
ALDH18A1	Aldehyde dehydrogenase 18 family member A1	Converts glutamate into pyrroline-5-carboxylate (P-5-C)
OAT	Ornithine Aminotransferase	Converts P-5-C into ornithine
ODC	Ornithine Decarboxylase	Converts ornithine to polyamines
SRM	Spermine Synthase	Converts ornithine to polyamines
SMS	Spermidine Synthase	Converts ornithine to polyamines

Supplemental Table 1. Description of glucose metabolism, glutaminolysis and polyamine synthesis genes by gene symbol, metabolic pathway and description of function. Related to Figures 2, 3, 4 and 5

Supplemental Figure 1

Log 2 Avg Normalized Reads

Monocytes

Gene	V1	V5
GLUT1	7.37	7.24
HK2	13.02	13.04
LDHA	13.70	13.67
PDHA1	10.90	11.01
SLC1A5	11.77	11.81
GLS	11.16	11.31

CD4 Tcells

Gene	V1	V5
GLUT1	10.54	10.53
HK2	9.67	9.98
LDHA	13.02	13.24
PDHA1	10.67	10.68
SLC1A5	8.65	9.43
GLS	12.32	12.81

Supplemental Figure 1: Presentation of Figure 2 data as Log 2 normalized reads. Related to Figure 2

Supplemental
Figure 2

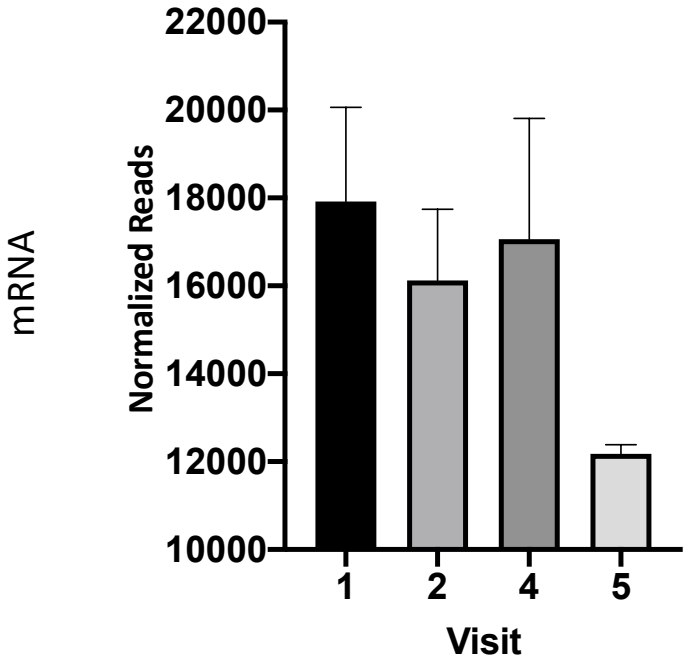

Supplemental Figure 2: **BCG vaccination reduces Dectin-1 transcription. Related to Figure 5A.** Longitudinal RNAseq analysis shows that CLEC7A (Dectin-1) transcription is reduced over time in monocytes isolated from BCG-vaccinated T1Ds (n=3). This indicates that BCG does not work via Dectin-1 as is the case for altered metabolism from **β**-Glucan .

Supplemental Figure 3

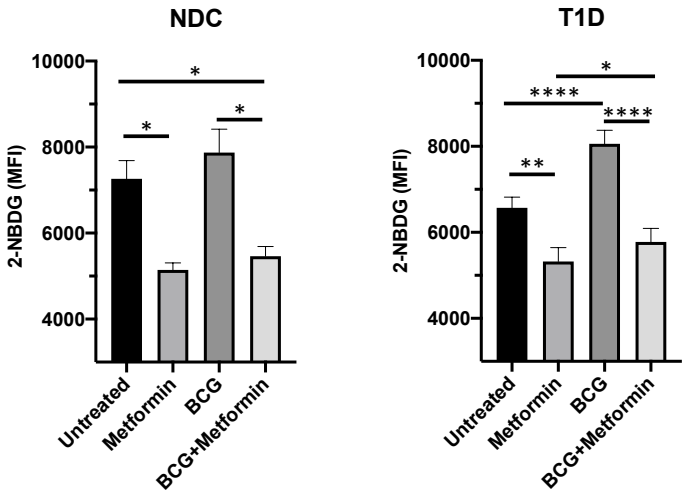

Supplemental Figure 3: **Metformin provides additional confirmation of the utilization of HIF-1a and mTOR for augmented MYC dependent glycolysis in T1D. Related to Figure 5A.**
In both NDC and T1D, metformin treatment reduces glucose transport as measured by 2-NBDG. Sugar transport, an indication of augmented aerobic glycolysis, is reduced. This reduction is partially corrected by BCG treatment concurrent with metformin. This demonstrates that BCG utilizes the AMPK, mTOR and HIF-1$\boldsymbol{\alpha}$ pathway for its signaling pathway. (NDC n=5; T1D n=16. Level of significance in figures is indicated by asterisk(s): * $p < 0.05$; ** $p < 0.01$; *** $p < 0.001$; **** $p < 0.0001$)

TRANSPARENT METHODS

STAR*METHODS

KEY RESOURCES TABLE

Reagent or Resource		
BCG	Japan BCG Laboratory, Tokyo, Japan	Freeze dried glutamate BCG vaccine (Japan) for intradermal use
2-NBDG	Thermo Fisher, Grand Island, NY	Cat# N13195
ImmunoCult-SF	Stemcell Technologies, Cambridge, MA	Cat# 10961
Metformin	Sigma Aldrich, St. Louis, MO	Cat# 317240
APC-anti CD14 antibody	BD Biosciences, San Jose, CA	Cat# 555399
EasySep Direct Human Monocyte Isolation Kit	Stemcell Technologies, Cambridge, MA	Cat# 19669
EasySep Direct Human CD4+ Tcell Isolation Kit	Stemcell Technologies, Cambridge, MA	Cat# 19662
PBS	Gibco/Thermo Fisher, Grand Island, NY	Cat# 20012-027
EDTA	Sigma Aldrich, St. Louis, MO	Cat# E-7889
Seahorse XF RPMI medium, pH 7.4	Agilent, Santa Clara, CA	Cat# 103576-100
Seahorse XFp Glycolytic Rate Assay Kit	Agilent, Santa Clara, CA	Cat# 103346-100
Seahorse XFp FluxPak	Agilent, Santa Clara, CA	Cat# 103022-100
Seahorse XFp Analyzer	Agilent, Santa Clara, CA	Cat# S7802A
CRL-9855 Cell Line	ATCC, Manassas, VA	Cell Line: CRL-9855
cMYC siRNA (Silencer™Select)	Thermo Fisher Scientific,	Cat# AM16708
Viromer®Green	Origene, Rockwille, MD	Cat# TT100301
c-MYC antibody	Bio-Rad, Hercules, CA	Cat# Clone 9E10
Cellular permeabilization buffe	BioLegend, San Diego, CA	Cat# 425401
Transcription Profiling analysis (RNAseq)		
RNeasy Plus Mini Kit	QIAGEN Sciences, Germantown, MD	Cat# 74104
2100 Bioanalyzer Instrument	Agilent, Santa Clara, CA	Cat# G2939BA
NEBNext® Poly(A) mRNA Magnetic Isolation Module	New England BioLabs, Ipswich, MA	Cat# E7490L
NEBNext® Ultra Directional RNA Library Prep Kit for Illumina	New England BioLabs, Ipswich, MA	Cat# E7420L
KAPABiosystems Illumina Library Quantification kit	KAPABiosystems, Wilmington, MA	Cat# KR0405
NextSeq 500 sequencer	Illumina Inc., San Diego, CA	Cat# SY-415-1002
TopHat	Johns Hopkins University, Center for Computational Biology	Open Source. Hosted at http://ccb.jhu.edu/software/tophat/index.shtml
Cufflinks	GitHub	Open Source. Hosted at https://github.com/cole-trapnell-lab/cufflinks
DESeq	Part of Bioconductor	Open Source. Hosted at https://www.bioconductor.org
Ingenuity Pathway Analysis	Qiagen BioInformatics, Redwood City, CA	https://www.qiagenbioinformatics.com/products/ingenuity-pathway-analysis/
Deposited Data		
RNASeq data	https://data.mendeley.com	http://dx.doi.org/10.17632/6frc2b83rv.1

CONTACT FOR REAGENT AND RESOUCE SHARING

Further information and requests for resources and reagents should be directed to and will be fulfilled by the Lead Contact, Denise L. Faustman (faustman@helix.mgh.harvard.edu).

DEPOSITED DATA

The normalized raw RNAseq data for the genes in this paper is deposited at http://data.mendeley.com and can be accessed using http://dx.doi.org/10.17632/x9kh4m22gy.1

EXPERIMENTAL MODEL AND SUBJECT DETAILS

Clinical trial and research study participants

All human studies had full institutional approvals through Massachusetts General Hospital and Partners Health Care (Study# 2007P001347, 2012P002243 and 2013P002633). The BCG interventional studies were also formally approved by the FDA (IND#2007P001347 and IND#2013P16434). All other blood donors both T1D and non-diabetic control (NDC) subjects consented through Study #2001P001379. Informed consent was obtained from all subjects and the experiments conformed to the principles set out in the WMA Declaration of Helsinki and the Department of Health and Human Services Belmont Report. The timing of BCG vaccinations and serial blood sampling times for visits 1 through visit 5 are depicted in Figure 1A. This study spanned 56 total weeks and includes type 1 diabetic patients with > 15 years of disease. All cohorts studied participated in open label studies conducted with serial BCG administrations and were not part of double blinded placebo controlled clinical trials.

Clinical chemistries

All human HbA1c, and glucose levels were determined directly from fresh blood by certified diagnostic laboratories approved by The Massachusetts General Hospital and the FDA. Human serum samples were assayed for C-peptide using regular (Cat# 10-1136-01) or ultrasensitive (Cat# 10- 1141-01) C-peptide ELISA kits from Mercodia AB (Uppsala, Sweden) using serum frozen at -80°C as previously described

(Faustman *et al*, 2012).

Isolation of monocytes and of CD4 T cells

Monocytes and CD4 cells were isolated from blood that was collected in purple tops (K_2-EDTA anticoagulant) using magnetic EasySep Direct Human Monocyte Isolation Kit or Easysep Direct Human CD4+ T Cell Isolation Kits from Stemcell Technologies (Vancouver, BC, Canada), following the instructions of the manufacturer. Briefly, 1200 µL of Isolation Cocktail and 1200 µL of RapidSpheres were mixed with 24 mL of whole blood in a 50 mL centrifuge tube and incubated for 5 min at room temperature. Twenty-four milliliter of Ca- and Mg-free PBS (for CD4 T cells) or PBS + 1mM EDTA (for monocytes) was then added and the tube placed into a "Easy 50" magnet (Stemcell Technologies). This immobilized the unwanted cells at the side of the tube. After 10 min, the monocyte- or CD4- enriched cell suspension was then transferred into a new tube and the magnetic separation process repeated for 5 min with fresh RapidSpheres. The resulting highly monocyte or CD4 enriched cell suspension was transferred into a new tube and purified for a third time using the magnet. The resulting final monocyte or CD4 T cell preparations had purities of >95%.

2-NBDG uptake in monocytes

Monocytes were isolated from T1D patients and cultured for 24 hours on Nunc UpCell 24-Well plates (Thermo Scientific, Cat# 174899) at a concentration of $1x10^6$ cells/mL in 1mL of Immunocult-SF Media (Stemcell Technologies), with or without $1x10^5$ CFU BCG added to the media (Multiplicity of Infection, MOI 0.1). Some cultures also included 1 mM metformin. UpCell plates have a coating that exhibits a temperature dependent transition from hydrophobic to hydrophilic. Thus, the coating allows cell attachment at 37°C whereas the cells will detach at room temperature or lower. In our experience this is the gentlest way to detach primary monocytes with minimal damage. Cells were recovered, washed, and incubated for 30 minutes at 37°C with 100uM 2-NBDG ((2-(*N*-(7-Nitrobenz-2-oxa-1,3-diazol-4-yl)Amino)-2-Deoxyglucose); ThermoFisher Cat# N13195) in Hepes buffered RPMI without glucose (XFp

medium, pH 7.4; Agilent Technologies, Wilmington, DE, USA. Cat# 103576-100). The cells were then washed with XFp medium and analyzed on a BD FacsCanto II flow cytometer. Data was processed using FlowJo software to determine 2-NBDG median fluorescence intensity (MFI).

Glycolytic Rate Assay

Changes in Oxygen Consumption Rate (OCR) and Extracellular Acidification Rate (ECAR) were measured using a Seahorse XFp Analyzer (Agilent). Isolated monocytes were cultured (2 x 10^5 per well) for seven days with or without 1 x 10^6 CFU of BCG (MOI=5) in Immunocult-SF Media (Stemcell Technologies). The cells were then washed with Seahorse XFp medium and analyzed using the Seahorse XFp Analyzer. After obtaining three baseline data points, Rotenone and AntiMycin A (final concentration, 0.5 uM) were added to the media to inhibit oxygen usage due to oxidative phosphorylation.

Transcription profiling analysis (RNAseq)

Total RNA was isolated from purified monocytes and CD4 T cells using the RNeasy Plus Mini Kit of QIAGEN (QIAGEN Sciences, MD, Cat# 74104) and processed by the CCCB (Center for Cancer Computational Biology) at Dana Farber Cancer Institute (Boston, Mass). RNA quality was determined using an Agilent 2100 bioanalyzer. RNA with a RIN value greater than 6 and less than 10% DNA contamination was used for library preparation. Using an input of 100 ng of total RNA, poly-A selection was performed using a NEBNext® Poly(A) mRNA Magnetic Isolation Module. The resulting mRNA was used for library preparation using the NEBNext® Ultra Directional RNA Library Prep Kit for Illumina®. The RNAseq libraries were run on a high sensitivity DNA chip on the Agilent 2100 Bioanalyzer, and the functional concentration of the library was determined through qPCR using the KAPA Biosystems Illumina Library Quantification kit. Libraries to be sequenced were pooled at a concentration of 2 nM, and were denatured and diluted to a final concentration of 2pM and loaded onto the Illumina NextSeq 500. Alignment of reads against reference genome HG19 was performed using TopHat and analyzed using Cufflinks. The resulting data was then normalized using DESeq, part of the R— Bioconductor

package. Normalized data were analyzed using the Ingenuity Pathway Analysis software from QIAGEN, the R Statistical Programming language.

cMyc silencing and analysis

CRL-9855 (ATCC, Manassas, VA), a cell line established from human monocytes, was seeded at a density of 1×10^6 cells in normal 24 well culture plate with or without 1×10^5 CFU of BCG (JAPAN BCG LABORATORY, Tokyo, Japan) in total 1mL normal medium; IMDM (Thermo Fisher Scientific, Waltham, MA) including 10% FBS (Merck Millipore, Darmstadt, Germany), 1% Penicillin Streptomycin (CORNING, Corning, NY), 1% HT supplement (Thermo Fisher Scientific) and 0.1% 2-mercaptoethanol (Thermo Fisher Scientific). After 3 days culture at 37℃, the cells were divided into double the number of wells with the medium. At day 5, the cells were collected and seeded at a density of 2×10^5 cells in total 500uL medium without antibiotics. Half of the wells with expanded cells were transfected by final dosage 1nM cMyc siRNA (Silencer™ Select, Thermo Fisher Scientific) with Viromer™ Green (ORIGENE, Rockville, MD) following the manufacture's protocol. The sequences of used siRNAs are following: 1) Sense (5'->3'), AGACCUUCAUCAAAAACAUtt; Antisense (5'->3'), AUGUUUUUGAUGAAGGUCUcg: 2) Sense (5'->3'), ACAGCCCACUGGUCCUCAAtt; Antisense (5'->3'), UUGAGGACCAGUGGGCUGUga. The other wells were used as control cells, which were transfected with negative control siRNA (Silencer™ Select, Thermo Fisher Scientific). Two days after the transfection, the cells were harvested, and used in the 2-NBDG assay or flow cytometry.

The silencing of cMyc was confirmed via flow cytometry (FACS canto Ⅱ, BD Bioscience, Franklin Lakes, NJ). Prior to cMyc staining, 1×10^6 cells were fixed and permeabilized with FoxP3 Fix/Perm Buffer (BioLegend, San Diego, CA) following the manufacture's protocol. The permeabilized cells were stained with Alexa Fluor 647 labeled-c-Myc antibody (Bio-Rad, Hercules, CA), analyzed in the flow cytometry and the fluorescent intensity (MFI) was evaluated via FlowJo software (BD Bioscience).

Statistical methods

Statistical significance was determined using the unpaired or paired two-tailed Student's t-test. Computations were performed using SAS version 9.4 (SAS Institute, Inc, Cary, NC), the R Statistical Computing Language, or in Microsoft Excel. Confidence levels were set to 0.05. Level of significance in Figures is indicated by asterisk(s): * $p < 0.05$; ** $p < 0.01$; *** $p < 0.001$; **** $p < 0.0001$